

DAMAGE DIAGNOSIS OF PONTE ROTTO, A ROMAN BRIDGE ALONG THE ANCIENT APPIA

Chiara GERMINARIO¹, Michele GORRASI¹, Francesco IZZO²,
Alessio LANGELLA^{1,3}, Marco LIMONGIELLO⁴, Mariano MERCURIO^{1,3},
Daniela MUSMECF⁵, Alfonso SANTORIELLO⁵, Celestino GRIFA^{1,3,*}

¹ Dipartimento di Scienze e Tecnologie - Università degli Studi del Sannio,
Via De Sanctis snc – 82100, Benevento, Italy

² Dipartimento di Scienze della Terra, dell'Ambiente e delle Risorse - Università degli Studi di Napoli Federico II,
Complesso Universitario di Monte Sant'Angelo, Via Cintia 26 – 80126, Napoli, Italy

³ Center of Research on Archaeometry and Conservation Science (CRACS) - Complesso Universitario di Monte
Sant'Angelo, Via Cintia 26 – 80126, Napoli, Italy

⁴ Dipartimento di Ingegneria Industriale - Università degli Studi di Salerno,
Via Giovanni Paolo II 132 - 84084 Fisciano, Italy

⁵ Dipartimento di Scienze del Patrimonio Culturale - Università degli Studi di Salerno,
Via Giovanni Paolo II 132 - 84084 Fisciano, Italy

Abstract

This paper describes the results of the damage diagnosis performed on Ponte Rotto, a Roman bridge on the ancient Appia way located close to the city of Benevento (southern Italy). Despite it can be considered one of the most important remains of this type of monument in Campania region, the bridge was abandoned for centuries, being in a rather poor state of conservation; therefore, an accurate damage diagnosis has been carried out using an interdisciplinary approach, in order to plan conservative, preventive and restoration work for the requalification of this archaeological heritage. Photogrammetric survey and damage diagnosis following the Fitzner's method allowed identifying and quantifying the geomaterials adopted for the construction of the bridge and the weathering forms affecting it. Georeferenced orthoimages permitted the mapping of their areal distribution, the definition of the damage categories, and the estimation of the linear and progressive damage indexes, that revealed a definitely bad conservation state.

Keywords: *Damage diagnosis; Fitzner method; Photogrammetric survey; Ponte Rotto; Via Appia.*

Introduction

Ponte Rotto (or Appian Bridge) crossed the Calore river close to the ancient town of Benevento, on the path toward ancient *Aeclanum* (southern Italy) (Fig. 1a). It was one of the most important bridges in Campania region, either for its geographic location, dimension, and architectonic value. Since Roman times, in fact, the bridge facilitated the crossing of the Calore river near the confluence with the Mele torrent and ensured the connection between the urban centre of *Beneventum* and the colony of *Aeclanum* on the Via Appia, the most important consular road connecting Rome to Brindisi.

Historical sources and architectural reconstructions account for a bridge composed of six or eight archways, for a total length of 170 m and a height of 13-14 m [1–5]. The preserved

* Corresponding author: celestino.grifa@unisannio.it

structures can be ascribed to a viaduct built with quadrangular pillars in *opus quadratum*, archways and head walls of gables in concrete covered by bricks. Unfortunately, only the western ramp on the left side of the Calore river, made of bricks and limestones blocks, and three pillars on the opposite bank and an archway, are nowadays preserved (Fig. 1b, c).



Fig. 1. Sketch map of Ponte Rotto location (modified from [33]); view of western (b) and eastern (c) side of Ponte Rotto.

Its construction started in 118 AD and was completed in 126 AD, when emperor Hadrian dictated renovation works for the consular road; however, it is supposed that the structure was preceded by a late republican construction (1st century BC) since the strategic role of the infrastructure within the ancient road system of the internal areas of Sannio [3]. Archaeological traces and historical sources (*Tabula Peutingeriana*) highlighted that a place of refreshment and assistance to travelers (*statio Calor flumen*) was here located in the Roman period [6].

The bridge was restored in Longobard Era, with the addition of concrete pillars aimed at supporting wooden arches that replaced the collapsed arcades [2]. This intervention, due to the state of degradation of the structure likely aggravated by floods and overflows of the Calore river, was no longer sufficient in Medieval times, when the crossing was moved on a smaller bridge built with recycled materials of the same Hadrian bridge [7–10].

However, the bridge has been abandoned for centuries, experiencing carelessness and weathering that have resulted in a bad state of conservation. Actually, the monument in 1980s

was interested by restoration and consolidation works with the addition of concrete pillar reinforcements [4].

Since 2011, within the research project called *Ancient Appia Landscapes* (AAL) aimed at reconstructing the landscapes and agrarian arrangements of the territory along this sector of the *Via Appia*, the investigation of Ponte Rotto has been carried out with the aim of studying, preserving and valorizing such important archaeological monument.

The multidisciplinary approach started with a photogrammetric survey of the bridge remains that produced a tridimensional model and georeferenced orthoimages, which were used for the mapping of lithotypes, weathering forms and damage categories. This model provides a general idea on the current conservation state of the bridge and may represent, at the same time, a valuable support to the conservation and protection works.

The paper describes the results of the damage diagnosis performed on Ponte Rotto remains situated on the right side of Calore river using the Fitzner's method; such a method permits the quantitative estimation of geomaterials used for the construction of the monument, weathering forms affecting it, the identification of the damage categories and the quantification of damage indexes that provide an overview of the conservation state of the studied monument. The results of surveying and analysis on the western ramp of the bridge are now being completed.

Experimental

In May 2017 the bridge was surveyed, and photogrammetric results were used for further lithological and damage evaluation via Fitzner and Heinrichs method. Details of the analytical approach adopted for the study are below reported.

UAV photogrammetric acquisition and processing

The tests and the renderings carried out on Ponte Rotto were intended to validate photogrammetric acquisitions from UAV (Unmanned Aerial Vehicle), namely a DJI Phantom 4, a drone that weighs about 1400 g, capable of shooting video in 4K up to 30 frame per second and streaming HD videos on smartphones, tablets and external devices through a special App (DJI Go).

The camera is equipped with a 12 MPixel Sony Exmor sensor (size 6.3 x 4.7 mm sensor, pixel size 1.56 μm), which has a wide-angle lens with a 4 mm focal length and FOV (Field of View) of 94°. The camera integrated in the gimbal maximizes the stability of the images during the shooting.

In order to control the metric error six Ground Control Points (GCP) were taken on the arena floor by a Global Navigation Satellite System (GNSS) Geomax Zenith 25 used in RTK (Real Time Kinematic) mode. The accuracy of planimetry is below 1 cm and 2.5 cm for altimetry. Photogrammetric shots were acquired by manual mode since the presence of obstacles on the side of the bridge.

Three flights and a total of 273 images were planned, according to 3 consecutive strips, acquired in time-lapse mode (5 s interval). In the first flight, 74 photographic shots were acquired in nadir mode (NW-SE direction, average height 19 m, ground coverage of about 29.9 x 22.3 m). Two other flights, with the camera tilted at 45° on the horizontal plan, were carried out acquiring, respectively, other 96 and 106 photos (17 m and 9 m on both sides; the ground coverages of about 26.8 x 20 m and 14.2 x 10.6 m, respectively) [11].

An Agisoft PhotoScan, 1.3.2 build 4164 version, was used for data treatment. The following parameters were set for the calculation of point clouds: in the Align Photos phase, Accuracy = High (original photos), Key-Point limit = 40000, TiePoint limit = 40000. To optimize camera alignment process, f (focal length), cx and cy (principal point offset), k1, k2, k3, k4 (radial distortion coefficients), were fitted. In the building of the Dense Cloud the parameters used were: Quality = High (1/4 of original photos), Depth filtering = Disabled.

Once completed the photogrammetric shots, the texturized 3D model of Ponte Rotto was created, the nadiral extracted, as well as the west and east orthophotos, required for the damage diagnosis. For the photogrammetric elaboration, all the points measured on the ground were used as GCPs [12].

The GNSS-NRTK survey was performed by a dual frequency Geomax Zenith 25. Horizontal coordinates were referenced to UTM Zone 33N (ETRF00), while the vertical values were also referred to ellipsoidal height.

Damage diagnosis

An accurate damage diagnosis has been performed on the central arcade and the two lateral pillars of Ponte Rotto as they represented the best preserved part of the monument. Damage diagnosis was carried out according to the widely-accepted quantitative approach proposed by Fitzner and Heinrichs [13–15]. Starting from an accurate anamnesis of the monument, this method takes in account the distribution of geomaterials, weathering forms, and damage categories for the evaluation of conservation state by means of their accurate mapping.

Geomaterials have been identified by in-situ surveys, weathering forms has been classified according to ICOMOS-ISCS [16] and UNI 11182 [17] recommendations, whereas damage categories have been defined according to the classification schemes proposed by Fitzner and Heinrichs [30], who indicate that the decay intensity has to be attributed considering both qualitative and quantitative parameters. Six damage categories can be definitively determined and mapped. Two damage indexes, namely linear damage index (DI_{lin}) and progressive damage index (DI_{prog}) are finally calculated [13,15]; DI_{lin} represents an average of damage categories whereas progressive damage index emphasises the higher ones. They range from 0 to 5 and are calculated according to the following equations, respectively:

$$DI_{lin} = [B + (C * 2) + (D * 3) + (E * 4) + (F * 5)]/100 \quad (1)$$

$$DI_{prog} = \sqrt{[B + (C * 4) + (D * 9) + (E * 16) + (F * 25)]/100} \quad (2)$$

where B = percentage area of damage category 1, C = percentage area of damage category 2, D = percentage area of damage category 3, E = percentage area of damage category 4 and F = percentage area of damage category 5.

Results and discussion

Photogrammetric surveying

A 3D model of the bridge was generated from the elaboration of photogrammetric shoots, both as a point cloud and mesh model. Nadiral and lateral flights permitted the acquisition of 273 images arranging the camera in different positions (Fig. 2). An 8 million points cloud has been obtained for the complete surveying of the monument.

Dense Cloud has been generated (Fig. 3), as well as the polygonal model (Fig. 4a) and the Digital Elevation Model (DEM) of Ponte Rotto (Fig. 4b). The model is rather accurate, showing an average error on GPC lower than 4 cm [11,18].

Completeness of data acquired and the appropriate resolution permitted the extraction of good quality orthoimages from the point cloud model elaboration of photogrammetric data. Lateral orthophotos, extracted from the coloured model points selecting planes of projection parallel to the western and eastern fronts of Ponte Rotto (Fig. 5), were used for a quantitative evaluation of lithotypes and damage diagnosis, as also carried out for decay analysis of other important monuments (e.g. [19]).

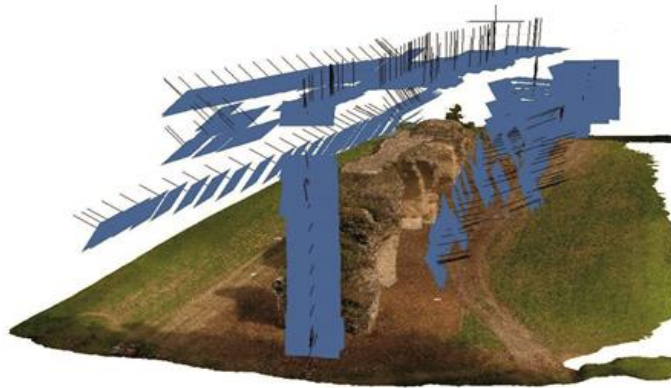


Fig. 2. Positions of camera during the flights of the drone.



Fig. 3. Perspective view of the arch of the bridge, obtained by the generated point cloud.

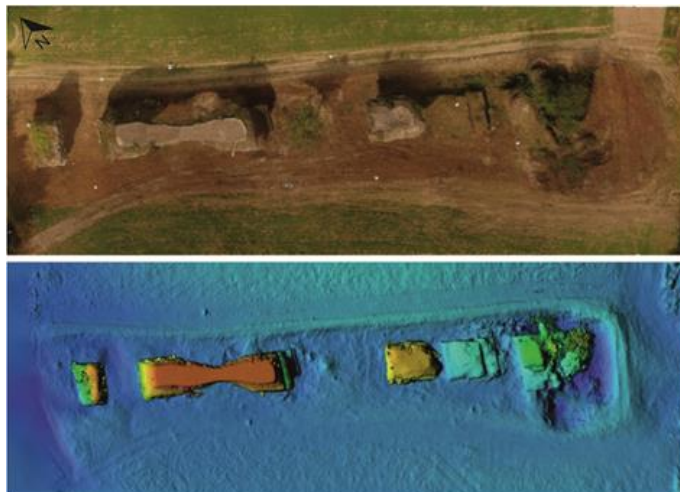


Fig. 4. Orthophoto (a) and Digital Elevation Model (b) of Ponte Rotto.



Fig. 5. Lateral orthoimages showing the western (a) e eastern front (b) of Ponte Rotto

Damage diagnosis

Geomaterials

The bridge was built with different techniques and geomaterials, as observed in other coeval monuments in Benevento [20], which basically depend on the structural function they had. Lithological mapping highlighted the presence of tuff material, bricks and limestones welded by mortars (Fig. 6; Table 1). Concrete, due to recent restoration works, also occur (Fig. 6).

Table 1. Geomaterials distribution

Façade		Tuff	Brick	Limestone	Cement	Mortar	Not observable	Total
Western	m ²	36.4	13.4	27.0	7.2	62.8	10.2	157.1
	%	23.2	8.5	17.2	4.6	40.0	6.5	100
Eastern	m ²	36.7	10.1	24.9	7.3	61.9	17.4	158.4
	%	23.2	6.4	15.7	4.6	39.1	11.0	100

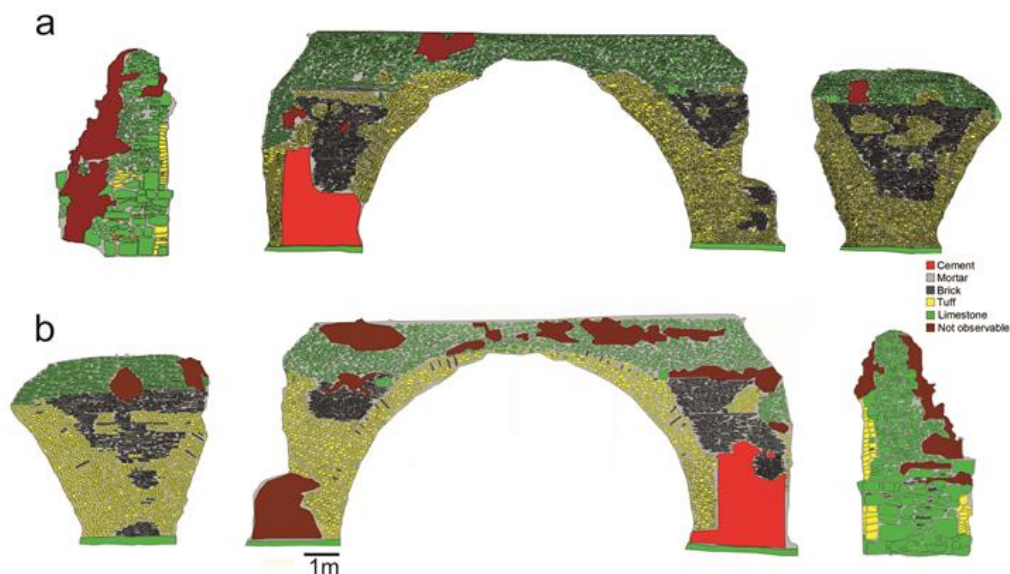


Fig. 6. Geomaterials distribution in western (a) and eastern (b) façade.

Yellow tuff material is the predominant building stone in both eastern and western façades (23.2%; Table 1), covering the lower part of the bigger lateral pillar and the central circular arch (Fig. 6). As also observed in nearby contexts [21], yellow tuff can be attributed to pyroclastic trachytic rocks (likely Campanian Ignimbrite in Yellow facies), one of the first building materials since Roman times, largely used for other coeval historical monuments of Campania region [22,23], also outcropping along the Calore river [24]. It is constituted by lithics, scoriae, pumices and crystals scattered in a cineritic yellow matrix which owes its color to post-depositional zeolitization processes [25,26]. Notwithstanding the widespread use in the building sector, its mineralogical properties made it suitable also in different industrial applications [25,27–31]. The framework of tuff blocks is made up in *opus incertum*, intercalated with bricks. Bricks (7.5% on average) were used as covering material in the upper part of all the elements of the bridge (arch and pillars; Fig. 6). They are generally horizontally oriented,

except for the archway where they signed the arch shape (Fig. 6). Bricks show a coarse-grained texture, with a temper mainly of volcanic origin (crystals and juveniles), mixed to siliciclastic grains scattered in the clayey matrix, in a mix-design consistent with coarse potteries and bricks from different buildings and archaeological sites in Benevento [20,32,33].

Limestones, occurring in different percentage on both sides (Table 1), have been recognized as large squared limestone blocks on the base of the pillars of the archway, and fluvial pebbles superimposed on the archway (Fig. 6). Geological availability in the surrounding areas [21], suggest that they could belong to the “Flysch Rosso” formation [24].

Mortar-based materials containing volcanic aggregate and covering around the 40% of the examined surfaces (Table 1) were used to bind the different building materials (Fig. 6). Such a mix-design of mortars is consistent with typical manufacturing techniques of Roman period [34–38], as also verified for other coeval monuments in Benevento [39].

Traces of the most recent reinforcement works were also detected such as a large concrete block used for the lateral pillar of the arch (4.6%; Table 1; Fig. 6)

A different framework was observed in the smaller lateral pillar (Fig. 6), made of large squared limestone blocks in *opus quadratum* along with larger tuff blocks (Fig. 6).

It should be remarked that a significant surface of the bridge (eastern façade 11.0%, western surface 6.5%) (Table 1) was not investigated due to the presence of plants mainly growing on the top and the bottom of the façades (Fig. 6).

Weathering forms

According to the classification schemes and nomenclature of weathering forms proposed by ICOMOS-ISCS [16] and UNI 11182 [17] recommendations, in-situ investigations allowed recognising 6 different types of weathering forms, gathered in three main groups (Table 2). Qualitative and quantitative intensity parameters are also reported (Table 2).

Table 2. Groups of weathering forms and intensity evaluation parameters.

Group of weathering form	Weathering form	Parameters of classification	Intensity	
			Low	High
GROUP III <i>Loss of material</i>	Missing part	Depth	< 3mm	> 3mm
GROUP IV <i>Discoloration and deposits</i>	Efflorescence	Surface covered	Partial	Total
	Patina	Surface darkness	Low	High
	Graffiti	Surface covered	Limited	Widespread
GROUP V <i>Biological colonization</i>	Plant	Surface covered	Partial	Total
	Lichen	Surface covered	Partial	Total

The missing parts represent the weathering form that extensively affects the bridge elements; it is generally due to the detachments of material from the upper part of the bridge (Fig. 7). The other types of weathering forms are related to the intrinsic properties of the building materials. For example, bricks are affected by efflorescences (Group IV), likely due to salts migrating from mortars to the pores of bricks through circulating aqueous solutions. Black patinas, instead, were mainly observed on the calcirudite and calcarenite pebbles on both façades (mainly in western façade; Fig. 7a) as a product of the natural decay of calcareous rock likely caused by the action of pollutants derived from urban and human activities [40].

Among the weathering forms of Group IV (discoloration and deposits) also graffiti have been observed on concrete blocks added during the consolidation works of 1980s (0.5 %; Table 2), attributed to an act of vandalism (Fig. 7a). The main weathering forms belonging to Group III (biological colonization) are represented by plants and lichens (Table 3; Fig. 7).

As described before, plants, located both on the upper and in the lower part of the bridge (Fig. 7) often hide the underlying structures. Moreover, roots provide serious structural damages, resulting in significant loss of material from the overall monument. Lichen colonization, instead, only affects the lower part of the pillars (0.4% on western façade, 2.2% on eastern façade; Table 3; Fig. 7); the latter, however, can be considered negligible since it does not imply direct decay effects.

Table 3. Weathering forms distribution

Façades		Western		Eastern		
Group	Weathering form	Intensity	%	m ²	%	m ²
III Loss of material	Missing part	Low	-	-	5.4	8.5
		High	30.6	48.0	21.6	34.3
	Efflorescence	Low	0.6	0.9	2.3	3.6
High		-	-	-	-	
IV Discoloration and deposits	Patina	Low	11.1	17.4	1.8	2.8
		High	2.9	4.5	1.9	3.0
	Graffiti	Low	0.5	0.8	-	-
		High	-	-	-	-
V Biological colonization	Lichen	Low	0.4	0.7	2.2	3.6
		High	-	-	-	-
	Plants	Low	4.1	6.5	9.7	15.3
		High	7.7	12.1	7.0	11.1
<i>Damaged surface</i>		<i>%-m²</i>	57.9	90.9	51.9	82.2
<i>Undamaged surface</i>		<i>%-m²</i>	42.1	66.2	48.1	76.2

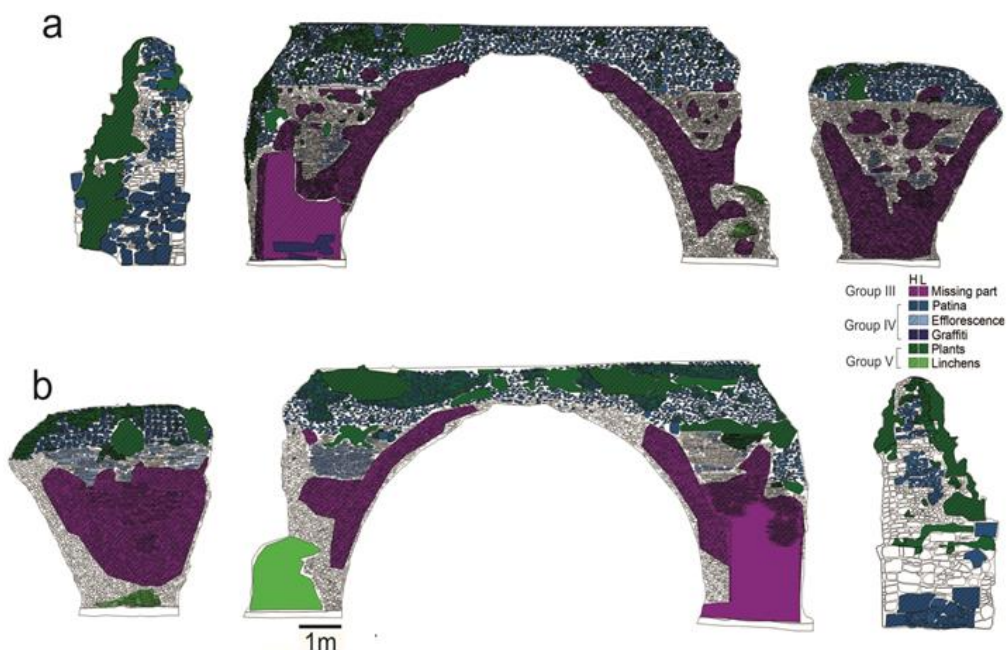


Fig. 7. Weathering forms distribution in western (a) and eastern (b) façade. Legend: H: high intensity; L: low intensity.

Damage categories and damage indexes

The correlation between the type of weathering forms recognised, their intensities and distribution, as well as the structural role of the damaged building materials, permitted an accurate damage diagnosis of Ponte Rotto [14,19]. Six different damage categories have been defined and quantified. The calculated damage indexes provide a reliable overview of the conservation state of the monument [13].

In general, Ponte Rotto is affected by a severe damage on both façades; actually, except for the areas affected by a very slight damage (Fig. 8), severe damage (damage category 4) affects a wide area of the analysed surfaces (29.1% on western façade, 30.1 % on western façade; Table 4). This situation appears more critical on the upper part of the bridge where different weathering forms (missing parts, patinas, plant invasions) are superimposed (Fig. 8). Moreover, in the central archway, a very severe damage (damage category 5) has also been recorded (Fig. 8), as the loss of materials provoked a noticeable and alarming thinning.

Table 4. Damage categories and damage indexes.

Damage categories	Western Façade (%)	Eastern Façade (%)
0 (no visible)	0	0
1 (very slight)	30.4	35.9
2 (slight)	26.9	22.1
3 (moderate)	12.3	10.8
4 (severe)	29.1	30.1
5 (very severe)	1.3	1.1
TOT (%)	100	100
DI_{lin}	2.44	2.38
DI_{prog}	2.73	2.70

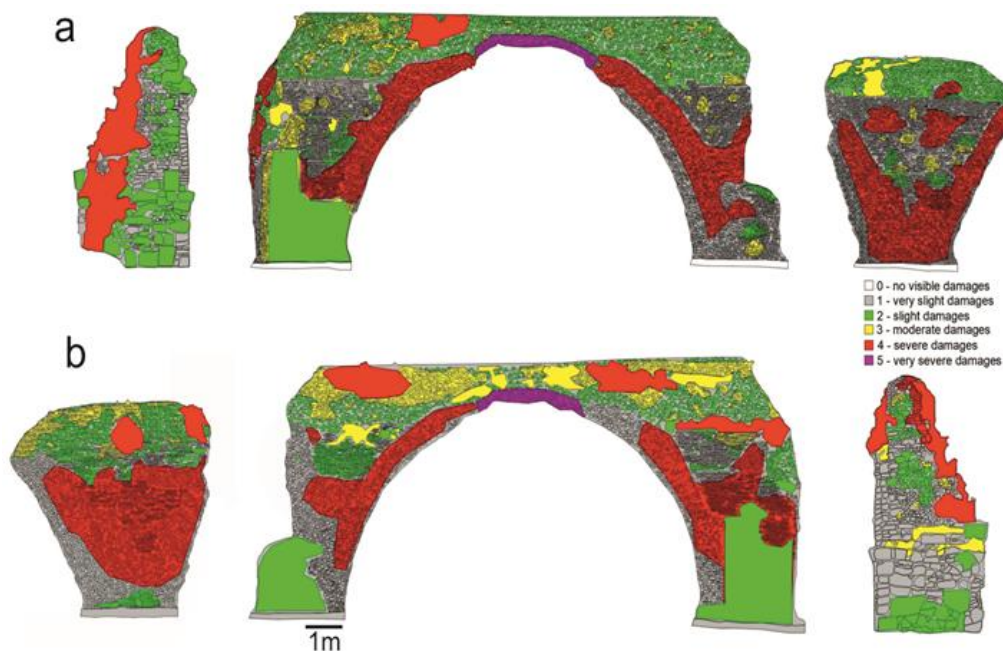


Fig. 8. Damage distribution in western (a) and eastern (b) façade

Roots of plants also determined a significant loss of material resulting in modest structural damages. For these areas, a damage category 3 (moderate) has been considered (12.3% on western façade, 10.8% on eastern façade; Fig. 8). Areas affected by black patinas, efflorescence and lichens colonizations, instead, were gathered in the damage category 2 (slight), as these weathering forms do not imply structural damages. For the same reason, graffiti were also considered a very slight damage pathology as it does not directly and significantly affect the conservation state of stone materials, except for its negative aesthetical impact (Fig. 8). Considering the global conservation state of the monument, a very slight damage category (damage category 1) was prudently attributed to the areas in which evident weathering forms were not detected (Fig. 8).

According to the proportion of the different damage categories, the damage indices DI_{lin} and DI_{prog} have been calculated. DI_{lin} on both facades suggest a rather severe damage (2.44 for western façade, 2.38 for eastern façade; Table 4), as well as the DI_{prog} which shows rather similar values (2.73 vs 2.70; Table 4). Such results describe a critical situation of the monument, making necessary potential monitoring and conservation works.

Conclusions

The present study, which is only a part of the wider research project *Ancient Appia Landscapes* focused on the territory along the route of the Via Appia close to the city of Benevento, reports the quantitative damage diagnosis of Ponte Rotto, an important archaeological heritage dated back to the Roman period and still preserved in this area. This research aimed at determining the current conservation state of the monument for planning conservative, preventive and restoration work in view of its requalification and valorization.

Damage diagnosis was carried out by means of a multidisciplinary approach that involved different expertise for a careful and quantitative determination of geomaterials, weathering forms and damage categories.

Fast and precise photogrammetric survey by drone provided a precise support for lithological and damage mapping; building materials reflected the local availability of lithotypes and the local building traditions. Yellow Phlegraean tuffs and calcareous stones outcropping in the surrounding areas have been adopted as building materials for this bridge, along with bricks. Building stones were jointed by mortar-based materials manufactured according to the usual ancient Roman technology.

Despite previous consolidation works performed in 1980s, building materials are affected by missing parts that cause the most important problems to the structural stability of the bridge, mainly when plant invasions also occur. Patinas of calcareous blocks have been observed, as well as lichens colonizations and graffiti. Water circulation, instead, favoured the deposition of salts on the bricks that caused the efflorescence phenomena. The mapping of weathering forms and the quantification damage categories and indexes highlight the damaged areas, showing a quite poor state of conservation.

This study represents an effective attempt of quantitative estimation of the conservation state of a large monuments that shed light on a rather critical situation; this result, in fact, not only may support the choice of the most adequate therapeutical actions for preserving the Ponte Rotto, but also can represent the first step in view of its requalification and valorisation.

Acknowledgments

The authors kindly thank the *Soprintendenza Archeologia belle arti e paesaggio delle province di Caserta e Benevento* and Dr. Simone Foresta, the municipality of Apice and the network of municipalities of *Via Appia Regina Viarium*. The authors are also grateful to Gaetano Memmolo for his support in the mapping procedures.

References

- [1] A. Meomartini, **I monumenti e le opere d'arte della città di Benevento: lavoro storico, artistico, critico**, Tipografia di Luidi De Martini e Figlio, Benevento, 1889, p. 503.
- [2] S. Aurigemma, *Apice. Iscrizione latina inedita riconosciuta in uno dei piloni di Ponterotto sul Calore e frammenti architettonici*, **Notizie degli scavi di Antichità**, 1911, pp. 355-359.
- [3] W. Johannowsky, *Fait partie d'un numéro thématique : Le Ravitaillement en blé de Rome et des centres urbains des débuts de la République jusqu'au Haut-Empire*, **Actes du Colloque international, Naples 14-16 Février 1991, 196** (1994), pp. 159-165.
- [4] L. Quilici, *Evoluzione tecnica nella costruzione dei ponti. Tre esempi tra età repubblicana e alto medioevo*, **Strade Romane, Ponti e Viadotti**, (Editors: L. Quilici, S. Quilici Gigli), L'Erma di Bretschneider, Roma, 1996: pp. 267-292.
- [5] V. Galliazzo, **I ponti romani**, Canova, 1995, p. 882.
- [6] S. Lo Pilato, *Il primo tratto irpino della via Appia*, **Via Appia Regina Viarum. Ricerche, contesti, valorizzazione**, (Editor: M. L. Marchi), Osanna Edizioni, Venosa, 2019, pp. 153-186.
- [7] A. Santoriello, A. Rossi, *Un progetto di ricerca tra topografia antica e archeologia dei paesaggi: l'Appia antica nel territorio di Beneventum*, **Proceedings of 3rd International Landscapes Archaeological Conference**, 2014: pp. 1-11.
- [8] A. Santoriello, C. De Vita, *Vivere in campagna lungo la via Appia: l'organizzazione e lo sfruttamento della terra tra IV sec. a.C. e VI sec. d.C. ad Est di Benevento*, **OTIVM. Archeologia e Cultura del Mondo Antico**, 4, 2018, 7.
- [9] A. Santoriello, *Archeologia dei paesaggi e strategie per la valorizzazione e la fruizione turistica in ambito rurale*, **ITALIA RURALE. Paesaggio, patrimonio culturale e turismo, IX Summer School Emilio Sereni - Storia del paesaggio agrario italiano** (Editors: G. Bonini, R. Pazzagli), Edizioni Istituto Alcide Cervi, Gattatico, 2018, pp. 203-216.
- [10] A. Santoriello, D. Musmeci, *La via Appia a Benevento (Beneventum – Calor fl.): dalla ricerca alle Comunità*, **Via Appia Regina Viarum. Ricerche, contesti, valorizzazione**, (Editor: M. L. Marchi), Osanna Edizioni, Venosa, 2019, pp. 69-89.
- [11] M. Limongiello, A. Santoriello, G. Schirru, R. Bonaudo, S. Barba, *The Amphitheatre of Avella: from its origin to digital*, **II° International Conference Metrology for Archaeology, MetroArchaeo 2016**, ISBN1 978-92-990075-4-9.
- [12] S. Barba, M. Barbarella, A. Di Benedetto, M. Fiani, M. Limongiello, *Comparison of UVAS performance for a Roman Amphitheatre survey: the case of Avella (Italy)*. **The International Archives of the Photogrammetry, Remote Sensing and Spatial Information Sciences**, XLII-2, 11, pp. 179-186.
- [13] B. Fitzner, K. Heinrichs, D. La Bouchardiere, *Damage index for stone monuments, Protection and Conservation of the Cultural Heritage of the Mediterranean Cities*, **Proceedings of the 5th International Symposium on the Conservation of Monuments**

- in the Mediterranean Basin, Sevilla, Spain, 5-8 April 2000** (Editors: E. Galan, F. Zezza), Swets & Zeitlinger, Lisse, The Netherlands, 2002, pp. 315–326.
- [14] B. Fitzner, *Documentation and evaluation of stone damage on monuments*, **Proceedings of the 10th International Congress on the Deterioration and Conservation of Stone**, 2004, pp. 677–690.
- [15] B. Fitzner, K. Heinrichs, *Damage diagnosis at stone monuments - Weathering forms, damage categories and damage indices*, Understanding and managing stone decay- Proceedings of the International Conference "Stone weathering and atmospheric pollution network (SWAPNET 2001)" (Editors: R. Prikryl, H.A. Viles), Prague: The Karolinum Press, Praha, 2001, pp. 11–56.
- [16] ***, **Illustrated Glossary on Stone Deterioration Patterns**, ICOMOS-ISCS, Champigny Marne, France, 2008, p.79.
- [17] ***, **Materiali lapidei naturali ed artificiali. Descrizione della forma di alterazione - Termini e definizioni**, UNI 11182, Roma, 2006, p. 33.
- [18] S. Barba, M. Limongiello, F. Mele, *Uno strumento UAV sperimentale per una metodologia sempre più consolidata: il caso di Via di Nocera a Pompei*, **Memorias 18 CCIA La Habana CUJAE - Ministerio de Educación Superior**, 2016, pp. 1–14.
- [19] C. Grifa, S. Barba, F. Fiorillo, C. Germinario, F. Izzo, M. Mercurio, D. Musmeci, A. Potrandolfo, A. Santoriello, P. Toro, A. Langella, *The domus of Octavius Quartio in Pompeii: damage diagnosis of the masonries and frescoed surfaces*, **International Journal of Conservation Science**, **7**, 2016, pp. 885–900.
- [20] C. Grifa, V. Morra, A. Langella, *Caratterizzazione mineralogica e petrografica dei laterizi storici della città di Benevento*, **Costruire in "pietra" fra innovazione e tradizione - International Conference and Exhibition-CITTAM 2007**, Luciano Editore, Napoli, 2007, pp. 176–186.
- [21] F. Cilenti, A. Furno, C. Germinario, C. Grifa, F. Izzo, M. Mercurio, A. Langella, *Preliminary contribution on the conservation state of the domus domini imperatoris Apicii built by Frederick II along the Ancient Via Appia (southern Italy)*, **Convegno Tematico AIAR - Dalla Conoscenza alla Valorizzazione: il Ruolo dell'archeometria nei Musei**, Reggio Calabria, 27-29 Marzo 2019.
- [22] V. Morra, D. Calcaterra, P. Cappelletti, A. Colella, L. Fedele, R. de' Gennaro, A. Langella, M. de'Gennaro, M. Mercurio, *Urban geology: relationships between geological setting and architectural heritage of the Neapolitan area*, **Journal of the Virtual Explorer**, **36**, 2010, 3.
- [23] M. de'Gennaro, D. Calcaterra, A. Langella, **Le pietre storiche della Campania: dall'oblio alla riscoperta**, Luciano Editore, 2013, p. 384.
- [24] S. Vitale, S. Ciarcia, *Tectono-stratigraphic setting of the Campania region (southern Italy)*, **Journal Maps**, **14**, 2018, pp. 9–21.
- [25] P. Cappelletti, G. Cerri, A. Colella, M. de'Gennaro, A. Langella, A. Perrotta, C. Scarpati, *Post-eruptive processes in the Campanian Ignimbrite*, **Mineralogy and Petrology**, **79**, 2003, pp. 79–97.
- [26] A. Langella, D.L. Bish, P. Cappelletti, G. Cerri, A. Colella, R. de' Gennaro, S.F. Graziano, A. Perrotta, C. Scarpati, M. De'Gennaro, *New insights into the mineralogical facies distribution of Campanian Ignimbrite, a relevant Italian industrial material*, **Applied Clay Science**, **72**, 2013, pp. 55–73.
- [27] M. Mercurio, P. Cappelletti, B. de' Gennaro, M. De Gennaro, F. Bovera, F. Iannaccone, C.

- Grifa, A. Langella, V. Monetti, L. Esposito, *The effect of digestive activity of pig gastrointestinal tract on zeolite-rich rocks: An in vitro study*, **Microporous Mesoporous Materials**, **225**, 2016, pp. 133–136.
- [28] F. Izzo, M. Mercurio, B. de' Gennaro, P. Aprea, P. Cappelletti, A. Daković, C. Germinario, C. Grifa, D. Smiljjanic, A. Langella, *Surface modified natural zeolites (SMNZs) as nanocomposite versatile materials for health and environment*, **Colloids and Surfaces B: Biointerfaces**, **182**, 2019, pp. 62–79.
- [29] M. Mercurio, F. Izzo, A. Langella, C. Grifa, C. Germinario, A. Dakovic, P. Aprea, R. Pasquino, P. Cappelletti, S.F. Graziano, B. de'Gennaro, *Surface-modified phillipsite-rich tuff from the Campania region (southern Italy) as a promising drug carrier: An ibuprofen sodium salt trial*, **American Mineralogist**, **103**, 2018, pp. 700–710.
- [30] M. Mercurio, A. Langella, P. Cappelletti, B. de Gennaro, V. Monetti, M. de' Gennaro, *May the use of Italian volcanic zeolite-rich tuffs as additives in animal diet represent a risk for the human health?*, **Periodico Di Mineralogia**, **81**, 2012, pp. 393–407.
- [31] M.D. Jackson, S.R. Mulcahy, H. Chen, Y. Li, Q. Li, P. Cappelletti, H.-R. Wenk, *Phillipsite and Al-tobermorite mineral cements produced through low-temperature water-rock reactions in Roman marine concrete*, **American Mineralogist**, **102**, 2017, pp. 1435–1450.
- [32] C. Grifa, G. Cultrone, A. Langella, M. Mercurio, A. De Bonis, E. Sebastián, V. Morra, *Ceramic replicas of archaeological artefacts in Benevento area (Italy): Petrophysical changes induced by different proportions of clays and temper*, **Applied Clay Science**, **46**, 2009, pp. 231–240.
- [33] C. Germinario, G. Cultrone, A. De Bonis, F. Izzo, A. Langella, M. Mercurio, V. Morra, A. Santoriello, S. Siano, C. Grifa, *The combined use of spectroscopic techniques for the characterisation of Late Roman common wares from Benevento (Italy)*, **Measurement**, **114**, 2018, pp. 515–525.
- [34] F. Izzo, A. Arizzi, P. Cappelletti, G. Cultrone, A. De Bonis, C. Germinario, S.F. Graziano, C. Grifa, V. Guarino, M. Mercurio, V. Morra, A. Langella, *The art of building in the Roman period (89 B.C. - 79 A.D.): Mortars, plasters and mosaic floors from ancient Stabiae (Naples, Italy)*, **Construction and Building Materials**, **117**, 2016, pp.129–143.
- [35] C. Rispoli, A. De Bonis, R. Esposito, S.F. Graziano, A. Langella, M. Mercurio, V. Morra, P. Cappelletti, *Unveiling the secrets of Roman craftsmanship: mortars from Piscina Mirabilis (Campi Flegrei, Italy)*, **Archaeological and Anthropological Science**, **12**, 8, 2020.
- [36] C. Rispoli, A. De Bonis, V. Guarino, S.F. Graziano, C. Di Benedetto, R. Esposito, V. Morra, P. Cappelletti, *The ancient pozzolanic mortars of the Thermal complex of Baia (Campi Flegrei, Italy)*, **Journal of Cultural Heritage**, **40**, 2019, pp. 143-154.
- [37] C. Di Benedetto, S.F. Graziano, V. Guarino, C. Rispoli, P. Munzi, V. Morra, P. Cappelletti, *Romans' established skills: Mortars from D46b mausoleum, porta mediana necropolis, Cuma (Naples)*, **Mediterranean Archaeology and Archaeometry**, **18**, 2018, pp. 131–146.
- [38] C.M. Belfiore, M.F. La Russa, D. Barca, G. Galli, A. Pezzino, S.A. Ruffolo, M. Viccaro, G. V Fichera, *A trace element study for the provenance attribution of ceramic artefacts: the case of Dressel 1 amphorae from a late-Republican ship*, **Journal of Archaeological Science**, **43**, 2014, pp. 91–104.
- [39] F. Izzo, C. Grifa, C. Germinario, M. Mercurio, A. De Bonis, L. Tomay, A. Langella, *Production technology of mortar-based building materials from the Arch of Trajan and*

- the Roman Theatre in Benevento, Italy*, **The European Physical Journal Plus**, **133**, 2018, pp. 363.
- [40] F. Corvo, J. Reyes, C. Valdes, F. Villaseñor, O. Cuesta, D. Aguilar, P. Quintana, *Influence of Air Pollution and Humidity on Limestone Materials Degradation in Historical Buildings Located in Cities Under Tropical Coastal Climates*, **Water Air and Soil Pollution**, **205**, 359, 2009.
-

Received: December 20, 2019

Accepted: February 26, 2020